Characterization of the fluidization of medium consistency pulp suspensions in a centrifugal pump

D. X. Ye, H. Li, C. H. Zou & B. Jiang
National Research Center of Pumps and Pumping System Engineering and Technology, Jiangsu University, China

Abstract

Medium consistency technology was used to pump, stock, beat, bleach and filter pulp suspensions at a medium concentration in the papermaking industry. When the concentration exceeds 5%, it stops flowing and acts like a solid. An important property of the fluidization of pulp suspension permits the use of centrifugal pump to transport pulp suspension. Based on the experimental data of medium consistency pulp suspension, the Herschel–Buckley model of non-Newtonian fluid was modified. The rheological behavior of the pulp suspension, bleached softwood kraft pulp suspension (SBK), hardwood pulp suspension (HW), thermal mechanical pulp suspension (TMP), and stone ground wood pulp suspension (SGW) in a medium consistency pump (MC pump) with a turbulence generator were simulated using computational fluid dynamics (CFD) software. A modified Herschel–Buckley model was used to approximate rheological behaviors of medium consistency pulp fibre suspension. The effects of shear stress, pump speed, fluid rheology, and the onset of fluidization were explored in the turbulence generator.
Keywords: fluidization, rheology, pulp suspensions, centrifugal pump.

1 Introduction

The rheology behaviors of pulp fibre suspension exhibit as Yield-pseudoplasic fluids [1]. When the imposed shear stress is beyond the threshold value, pulp suspensions start flowing because networks build up, just like a solid body, at low shear rates and break down at high shear rates. The fluidization of medium consistency pulp suspension mass concentrations ($Cm = 5$–20%) can only be attained in turbulent state and the apparent yield stress must be exceeded.

Gullichsen and Harkonen (1981) [2] pioneered the use of fluidization can pump medium consistency pulp fibre suspensions. Bennington *et al.* (1991) [3] and Bennington and Kerekes (1996) [4], and Hietaniemi and Gullichsen (1996) [5] researched that fluidization could occur at loc level and fibre level because of large difference in their apparent yield stress. The latter studies measured the onset of fluidization, defining the onset of fluidization is common for turbulence flow in mixing vessels.

Medium consistency technology (MC technology) was first developed in northern Europe in 1970s. Medium consistency technology was used to pump, stock, beat, bleach and filter pulp suspensions at medium concentration. MC technology is efficiency, low energy consumption and less pollution technology, so MC technology will be in place of low medium consistency technology. The fluidization of pulp suspensions is an essential operation to transport suspension in centrifugal pump. One of the important equipment in medium consistency pump is turbulence generator, which is indispensable to fluidization in pump process.

The rheology behaviors of pulp suspension are often characterized by the power number, N_p, is the ratio of shaft power to speed, turbulence generator diameter. The stress, τ, is the ratio of shaft torque to radius of turbulence generator, the vane height:

$$Np = \frac{P}{\rho N^3 D^5} \tag{1}$$

$$\tau = \frac{M}{2\pi R^2 h} \tag{2}$$

where $P = 2\pi NM$

As turbulence equipment and axial flow impeller, the turbulence generator is designed for agitation and fluidization. The N_f is often used to describe axial flow impeller thrust number. The axial flow impeller number is the ratio of axial thrust to shaft speed, the turbulence generator diameter:

$$N_f = \frac{F_A}{\rho N^2 D^4} \tag{3}$$

with P being the shaft power draw, N the shaft speed, M the shaft torque, ρ the pulp density, D the turbulence generator diameter, R the radius of turbulence generator, h the vane height, F_A the axial thrust.

In this paper, the Herschel–Buckley model of non-Newtonian fluid was modified, and the characterization of medium consistency fibre pulp suspension in centrifugal pump with turbulence generator were studied.

2 Structure of the medium consistency pump with a turbulence generator

Figures 1 and 2 show a schematic diagram of the structure of medium consistency pump. The duty point of the pump is at a flow rate of 600 m³/h, a head of 120 m,

a efficiency of 52.1%. The rotational speed is 1450rpm. The turbulence generator consists of four shear-twisted blades, and the diameter D is 257 mm. The vane height h is 260 mm. Before medium consistency fibre suspension flows into impeller, it consists of eight blades, the medium consistency fibre pulp must be fluidized. When MC pump starts and shaft is in rotation, the medium consistency pulp will be brought in turbulence generator, and enough shear force imposes on pulp suspension, so the medium consistency pulp is in turbulence state after turbulence generator. The pulp suspension will flow along dashed line through the pump.
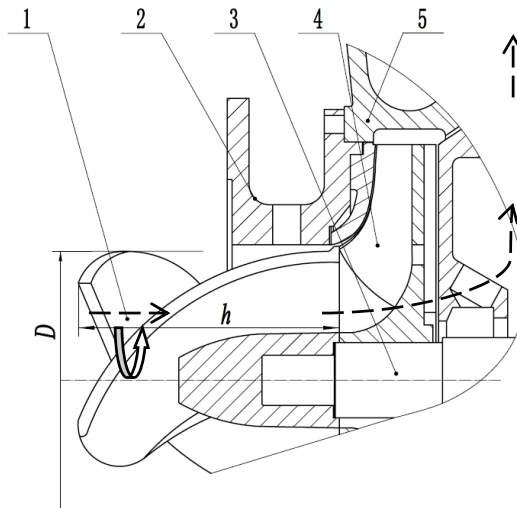

Figure 1:   The structure of medium consistency pulp pump. 1. Turbulence generator; 2. Pump flange; 3. Shaft; 4. Impeller; 5. Volute.
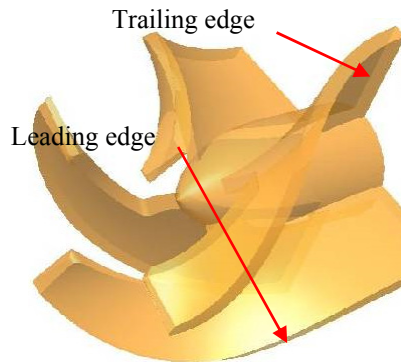

Figure 2:   The 3D turbulence generator.

3   CFD simulations

Characterization of fluidization of medium consistency pulp suspensions can be time consuming and expensive in centrifugal pump in experiment. In this regard, a commercial CFD software (CFX) was employed to model the pulp suspension flow field and solve the momentum and continuity equations in the laminar regime, because of the pulp flow is in laminar state before fluidization. The computational domain in centrifugal pump was discretized with robust unstructured tetrahedral mesh using ANSYS-ICEM. The mesh quality has a significant effect on the accuracy of numerical results, and the quality of tetrahedral mesh, the minimum ratio of height to base length of each side tetrahedral grid, is above 0.2 and the mix-angel is larger than 18 degree. In general, the numbers of grid requires to be fine enough to calculate the flow details especially in some complex regime, but it is too fine to consume more time to solve the flow field. Mesh independency was check shown in table 1 by demonstrating that additional cell number did not change the N_p and N_f by more than 2% comparing to the fine cell number. Compared to fine cell, deviations of N_p and N_f are 2.88% and 1.82% for coarse cell, and there are only 1.43% and 0% for medium cell. The numbers of mesh with three-dimensional mesh of centrifugal pump is 1147250.

Table 1:   Mesh independency investigation.

Cell number	Turbulence generator	Impeller	Volute	N_p	N_f	Deviation of N_p and N_f /%
coarse	2.56×10^5	4.51×10^5	2.33×10^5	1.43×10^{-3}	1.12×10^{-3}	2.88, 1.82
medium	4.23×10^5	3.78×10^5	3.39×10^5	1.41×10^{-3}	1.10×10^{-3}	1.43, 0
fine	7.89×10^5	5.02×10^5	6.07×10^5	1.39×10^{-3}	1.10×10^{-3}	--

The frozen-rotor interface was used for connection, with coupling between stationary and rotational frame made using quality and velocity transformation. A no-slip wall condition was set at all boundaries, and a scalable wall- function was used to solve boundary layer field. As boundary conditions, a total pressure at inlet and an opening at outlet were defined. The CFD calculation is steady state.

A modified Herschel–Buckley model [6–9] was used to approximate rheological behaviors of the medium consistency pulp fibre suspension. The computation is instability because of the numerical problem at small shear rate for non-Newtonian Herschel–Buckley fluids. The pulp suspension acts as an extremely viscous fluid, μ_0 at $\tau \leq \tau_y$ and the rheology behavior is described as a power law model , H-B model, at $\tau > \tau_y$

$$\eta = \mu_0 \quad \text{for} \quad \tau \leq \tau_y \tag{4}$$

$$\eta = \frac{\tau_y + k[\dot{\gamma}^n - (\tau_y / \mu_0)^n]}{\dot{\gamma}} \quad \text{for} \quad \tau > \tau_y \tag{5}$$

with μ_0 the yielding viscosity, τ_y yielding stress, k consistency index, $\dot{\gamma}$ shear stress rate. Table 2 [10] shows the Herschel–Buckley models of medium pulp fibre suspension.

Table 2: Herschel-Buckley parameters for bleached softwood kraft pulp suspension (SBK), hardwood pulp suspension (HW), thermal mechanical pulp suspension (TMP), and stone ground wood pulp suspension (SGW) as functions of 5% consistency.

Pulp suspension	Yielding stress σ_y (Pa)	K (Pa.s)	n (-)
SBK	415±60	112±10	0.11±0.01
HW	173±12	84±6	0.13±0.02
TMP	251±24	76±5	0.13±0.03
SGW	143±18	62±12	0.14±0.02

The scaled residuals for each transport equations were below 1×10^{-5} of simulation was considered convergence. The turbulence generator torque and axial thrust force were calculated using pulp flow field, and this depended on the pulp properties and boundary conditions, especially the pulp fibre suspension viscosity. Near the turbulence generator maximum diameter flow regime the shear rate is high, and the viscosity of pulp suspension was calculated with equation 5.

4 Results and discussion

In this paper, the turbulence generator power number N_p and axial force number N_f for SBK, HW, SGW, and TMP pulp fibre suspensions at medium consistency $C_m=5\%$, the mass concentration of fibre mass divided by the sum of fibre mass and water, in centrifugal pump were showed in figure 3 and figure 4. Both of N_p and N_f dependence on N (rotational speed) indicate that suspension flows are in the laminar and transitional-to-turbulence regime when the power number curves approximated to horizon. N_p increased with different yield stress of pulp fibre suspension, and the number of power N_p curves decreases from SBK>TMP>HW≈SGW for a fixed rotational speed before 200rpm. With the speed increasing, all power number N_p decrease. Especially, the N_p of SBK pulp suspension is below all the others'.

Compared with N_p, it is different that the turbulence generator axial force number N_f curves collapse to a horizontal line after pulp fibre suspension yielded. Similar results are report for rheology properties of pulp fibre suspensions by Nagata (1975) [11], Ein-Mozaffari et al. (2003) [12], Prajapati and Ein-Mozaffari (2009) [13], Bhole et al. (2009) [9], and Gomez et al. (2010) [14].

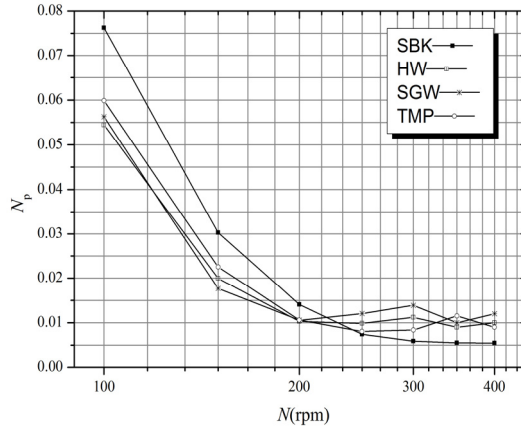Figure 3: Turbulence generator power number (N_p) versus rotational speed (N).
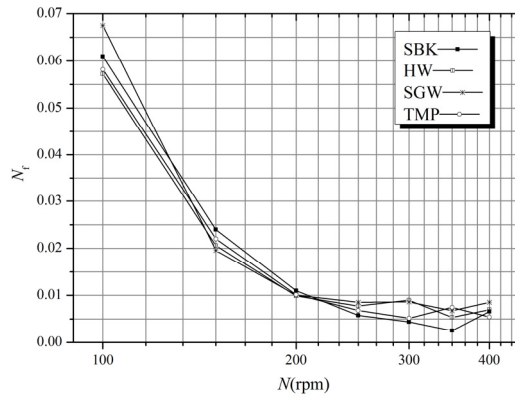

Figure 4: Turbulence generator axial force number (N_f) versus rotational speed (N).

Figures 5 and 6 show the power number (N_p) versus and axial force number (N_f) versus Reynolds number (Re) for the different pulp suspensions with turbulence generator in centrifugal pump. Where the Reynolds number, Re, is given by

$$Re = \frac{\rho N^2 D^2}{\tau_y} \tag{6}$$

The power number (N_p) and axial force number (N_f) fall along with the Reynolds number (Re) at $Re < 200$, and it indicates that the flow is at laminar or transitional-to-turbulence status. At $Re > 200$, N_p and N_f deviate to horizontal line, which implies that the flow field is at turbulence status.
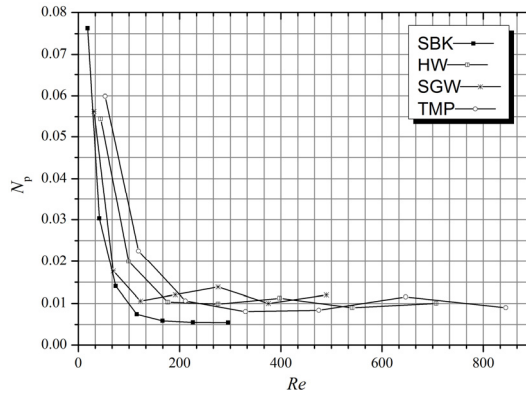
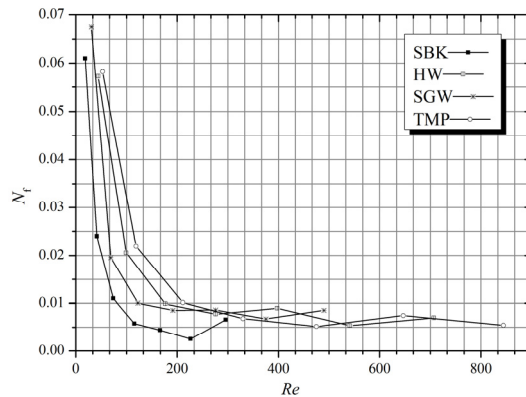Figure 5:   Turbulence generator power number (N_p) versus rotational speed (*Re*).

Figure 6:   Turbulence generator axial force number (Nf) versus rotational speed (Re).

Figure 8 shows the apparent dynamic viscosity of SBK, HW, TMP, and SGW pulp suspension in turbulence generator at N=200 rpm rotational speed on section plane shown in Figure 7. The flow is at transitional status. Because the turbulence structure results in low shear stress at leading of blade and the impeller blade effects the upstream field where it is trailing edge, it is found that almost large viscosity magnitude distributes between turbulence generator blades and there are two viscosity boundaries at inlet and outlet of generator. It was observed that the apparent viscosity magnitude decreased as the number of power N_p, and it is obviously that the apparent viscosity approached 4×10^5~5×10^5 Pa•s in TMP pulp fibre suspension. With the speed increasing, the shear stress increase, and the apparent dynamic viscosity of SBK reduces to 0.4 Pa•s at 400 rpm.
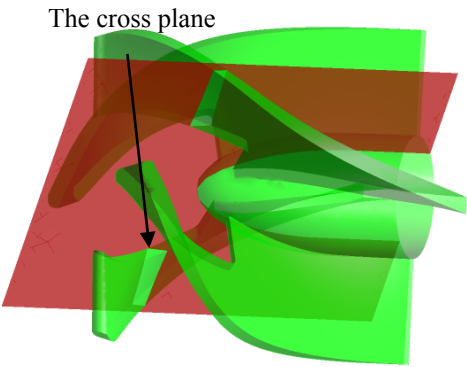
Figure 7: The cross plane on turbulence generator.

(a) SBK

(b) HW

(c) TMP

(d) SGW

(e) SBK at 400 rpm

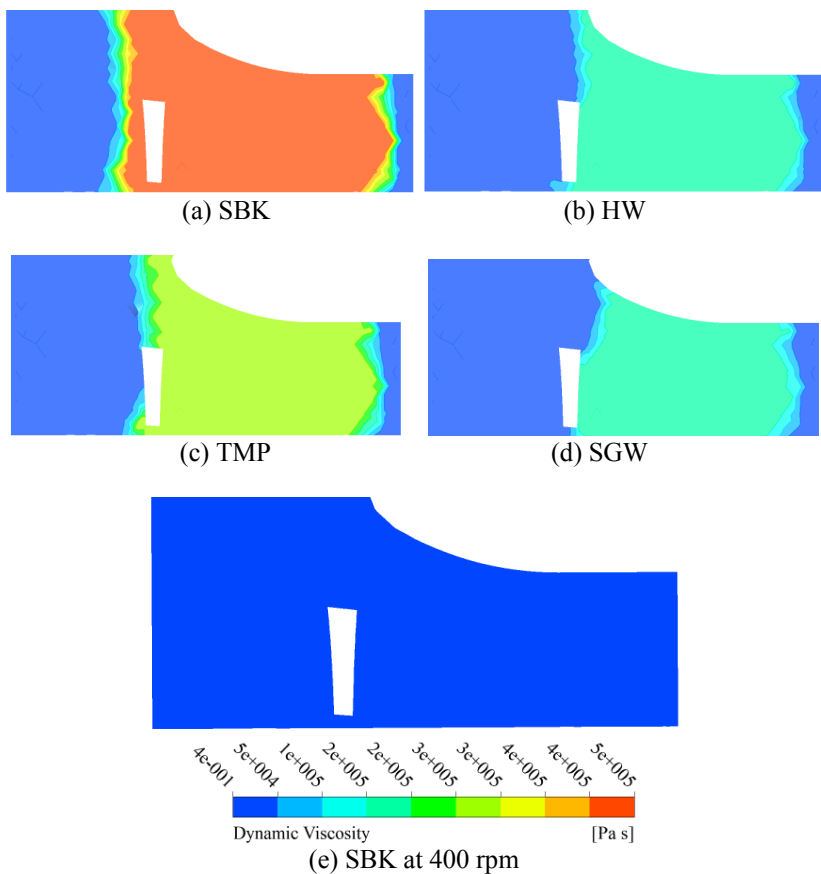Figure 8:   Apparent dynamic viscosities of SBK, HW, TMP, and SGW pulp
suspension at 200 rpm speed and SBK at 400 rpm.

5   Summary and conclusions

In this research, Herschel-Buckley parameters of experiment data for bleached softwood kraft pulp suspension, hardwood pulp suspension, thermal mechanical pulp suspension, and stone ground wood pulp suspension at 5% consistency were used to investigate. The rheology behaviors of pulp suspension which acts as Yield-pseudoplasic fluids. The power number, axial force number, Reynolds number and apparent viscosity were calculated and analyzed through the CFD technique at different rotational speed. The laminar to turbulence status were model at Herschel-Buckley model.

It is found that N_p and N_f decreased with rotational speed and Reynolds number increasing. The number of power N_p curves decreases from SBK>TMP>HW≈SGW for a fixed rotational speed before 200rpm. Pulp suspension flows are in transitional-to-turbulence status after $N = 200$ rpm and Re=200. Large viscosity magnitude distributes between turbulence generator blades. The apparent viscosity of TMP achieved $4\times10^5 \sim 5\times10^5$ P·as.

Nomenclature

C_m mass concentration (%)
N_p power number
P shaft power draw (W)
N shaft speed (rpm)
M shaft torque (N·m)
D turbulence generator diameter (mm)
R radius of turbulence generator (mm)
h vane height (mm)
F_A axial thrust (N)

Greek symbols
τ shear stress (Pa)
ρ pulp density (kg/m^-3)
μ_0 yielding viscosity (Pa•s)
τ_y yielding stress (Pa)
k consistency index
$\dot{\gamma}$ shear stress rate (s^-1)

Acknowledgements

References

[1]   C. W. Macosko, Rheology: Principles, Measurements and Applications, Wiley-VCH, New York 1994.

[2]   Gullichsen, J., Harkonen, E., 1981. Medium consistency technology. II. Storage dischargers and centrifugal pumps. Tappi Journal 64(6): 69-72.

[3]   Bennington, C.P.J., Kerekes, R.J., Grace, J.R., 1991. Motion of pulp fibre suspensions in rotary devices. Canadian Journal of Chemical Engineering 69(1): 251-258.

[4]   Bennington, C.P.J., Kerekes, R.J., 1996. Power requirements for pulp suspension fluidization. Tappi Journal 79(2): 239-275.

[5]   Hietaniemi, J., Gullichsen, J., 1996. Flow properties of medium consistency fibre suspensions. Journal of Pulp and Paper Science 22(12): 469-471.

[6]   Adams, L.W. and Barigou, M., 2007, CFD analysis of caverns and pseudo-caverns developed during mixing of non-Newtonian fluids. Chem Eng Res Des, 85: 598-604.

[7]   Arratia, P.E., Kukura, J., Lacombe, J. and Muzzio, F.J., 2006, Mixing of shear thinning fluids with yield stress in stirred tanks. AIChE J, 52: 2310–2322.

[8]   Kelly, W. and Gigas, B., 2003, Using CFD to predict the behavior of power law fluids near axial-flow impellers operating in the transitional regime. Chem Eng Sci, 58: 2141-2152.

[9]   M. Bhole, C. Ford, C. P. J. Bennington., 2009, Characterization of axial flow impellers in pulp fibre suspensions. Chem Eng Res Des, 87: 648-653.

[10] Derakhshandeh, B., Hatzikiriakos, S.G., Bennington, C.P.J., 2010. Rheology of pulp fibre suspensions using ultrasonic Doppler Velocimetry. Rheologica Acta 49(11-12): 1127-1140.

[11] Nagata, S., (1975). Mixing: Principles and Applications. Wiley, New York.

[12] Ein-Mozaffari, F., Dumont, G.A. and Bennington, C.P.J., 2003, Performance and design of agitated pulp stock chests. Appitata J, 56: 127-133.

[13] Poonam Prajapati, Farhad Ein-Mozaffari, 2009, CFD investigation of the mixing of yield-pseudoplastic fluids with anchor impellers. Chem, Eng. Technol, 32(8): 1211-1218.

[14] C. Gomez., B. Deraljsjandeh, S.G. Hatzikiriakos, C.P.J. Bennington. 2010, Carbopol as a model fluid for studying mixing of pulp fibre suspensions. Chemical Engineering Science. 65: 1288-1295.